Rojas-Lema, Gomez-Caturla, J., Balart, R., Arrieta, M. P., & Garcia-Sanoguera, D. (2024). Development and characterization of thermoplastic zein biopolymers plasticized with glycerol suitable for injection molding. Industrial Crops and Products, 218, 119035. https://doi.org/10.1016/j.indcrop.2024.119035

Development and characterization of thermoplastic zein biopolymers plasticized with glycerol suitable for injection molding.

S. Rojas-Lema[1], J. Gomez-Caturla[1], R. Balart[1], M.P. Arrieta[2,3], D. Garcia-Sanoguera[1]

[1] Instituto Universitario de Investigación de Tecnología de Materiales, Universitat Politècnica de València, ITM-UPV, Alcoy, Spain

[2] Departamento de Ingeniería Química Industrial y del Medio Ambiente, Escuela Técnica Superior de Ingenieros Industriales, Universidad Politécnica de Madrid ETSII-UPM, Spain

[3] Grupo de Polímeros, Caracterización y Aplicaciones (POLCA) Madrid, Spain.

Abstract.

This research focuses on the development of high environmentally efficiency materials based on zein plasticized with glycerol, processed through extrusion and injection molding techniques. The work addresses the study of the influence of glycerol content on the processability of thermoplastic zein (TPZ), as well as its effect on mechanical and thermomechanical properties, thermal transitions, degradation, microstructure, zein-plasticizer interactions, surface appearance, and wettability. The incorporation of glycerol facilitates the processing of thermoplastic zein. To process these materials through extrusion and injection molding, a minimum amount of 15 wt.% glycerol is required, while formulations with more than 40 wt.% glycerol expel part of the plasticizer through exudation. Through these processing techniques, it is possible to obtain thermoplastic zein with a tensile strength of up to 27.9 MPa, and elongation at break between 5-6%. The glass transition temperature, T_g, is significantly reduced from 43 ºC to values around 37 ºC, demonstrating the plasticizing efficiency that glycerol can exert on zein. This work demonstrates the feasibility of extrusion and injection molding processes for obtaining glycerol-

plasticized thermoplastic zein (TPZ), expanding the possibilities of zein use as a potential substitute of some petroleum-derived commodity plastics.

1. Introduction.

Nowadays, the use of sustainable eco-friendly materials from non-petroleum sources such as biopolymers or geopolymers has aroused enormous interest in society. Biopolymers come from renewable sources and are in some cases biodegradable, while geopolymers provide eco-friendly alternatives to conventional cement, emitting less CO_2 and utilizing abundant, low-cost materials (Kuang et al., 2022; Liu et al., 2023).

In this respect, Zein has garnered significant interest as a versatile biopolymer in recent years. Zein, found in maize endosperm cells, is a prolamin and an alcohol-soluble protein with a molecular weight of 20 kDa. Notably, zein contains, methionine and cysteine amino acids (Jaski et al., 2022), but it is deficient in essential amino acids like lysine and tryptophan, resulting in its limited nutritional value (Calvez et al., 2021; Gianazza et al., 1977). Zein is obtained as a by-product of the corn industry (Jiao et al., 2022); therefore, it has shown a great interest in the scientific community due to its excellent combination of properties which include, renewable origin, biocompatibility, biodegradability, low water-vapor permeability, non-toxicity, and amphiphilic character, among others (Kasaai, 2018; Zhang et al., 2021b). It is also considered as a generally recognized as safe (GRAS) biomaterial (Luo and Wang, 2014). Zein contains a large number of non-polar hydrophobic amino acid residues such as leucine, glutamine, proline, and alanine, which are responsible for it being insoluble in water (Giteru et al., 2021; Wang et al., 2015).

In recent years, zein-based materials have been proposed for a wide variety of biomedical applications. It has been used in controlled drug delivery since it is able to encapsulate bioactive compounds such as curcumin, α-tocopherol, vitamin D3, resveratrol, among others (Luo and Wang, 2014; Nunes et al., 2020; Raza et al., 2020; Zhang et al., 2021a). It has also found increasing applications as bioactive membranes for wound healing (Martin et al., 2022; Qin et al.,

2020), and scaffolds for tissue engineering due to its biocompatibility and ability to support cell growth (Pérez-Guzmán and Castro-Muñoz, 2020; Wu et al., 2012). Zein-based materials include a wide range of presentations, depending on the processing method. Zein-based inks can be 3D printed to create customized scaffolds for tissue engineering (Tavares-Negrete et al., 2021). Moreover, zein nanoparticles can be obtained by several methods such as antisolvent precipitation (Cui et al., 2021), emulsification (Pascoli et al., 2018), and coacervation (Kaushik et al., 2019), with application as carriers for controlled drug delivery of bioactive compounds (Peña-Bahamonde et al., 2023; Wang and Zhang, 2019). Zein-based nonentities can also be obtained by electrodynamic processes such as electrospinning and electrospraying with exceptional applications in tissue engineering, wound dressing, and drug delivery (Ghalei et al., 2018; Lenzuni et al., 2024). In addition, zein micro- and nanoparticles can be obtained by conventional drying methods (freeze drying, and spray drying), with applications in drug delivery systems (De Marco, 2022).

Zein has been developed in the field of food in the recent years (Jiang et al., 2023b) and has gained attention as a sustainable alternative for food packaging and edible films (Spasojevic et al., 2019; Tadele et al., 2023; Zhang et al., 2020). When plasticized, zein exhibits improved flexibility, barrier properties, and film-forming ability. Several plasticizers have been proposed, such as glycerol (Escamilla-García et al., 2013; Liang et al., 2015), polyethylene glycol (PEG) (Sun et al., 2020), oleic acid (OA) (Wang et al., 2003), deep eutectic solvents (Yilmaz et al., 2024), or mixtures, to reach synergistic effects (Xu et al., 2012; Zhou and Wang, 2021). In addition to its use as a plasticizer, glycerol has been widely used in a variety of other applications in sectors such as pharmaceuticals, coatings, food and cosmetics (Atta et al., 2022; Bangi et al., 2020; Li et al., 2022; Liu et al., 2022; Wang et al., 2022).

Although the use of zein as a biopolymer is well documented in the literature, it primarily involves the employment of this protein in the form of micro- and nanofibers, micro- and nanoparticles, films, and coatings (mainly obtained by the solvent cast process). There are not many studies focused on the use of zein in the manufacturing of thermoplastic zein (TPZ) through

conventional extrusion and injection processes, or other industrial processes, which could widen the use of zein in other applications. In some cases, it has been mixed with other biobased and/or biodegradable polymers. Masanabo *et al.* (Masanabo et al., 2022), developed starch-zein films with 25 wt.% processed by extrusion and compression molding. Selling (Selling, 2010), studied the effect of the processing temperature by extrusion of zein plasticized with triethylene glycol (TEG) and water, concluding mechanical properties of thermocompressed samples decrease above 140 ºC extrusion temperature. They also reported the effect of reactive extrusion of zein with glycerol and triethylene glycol (TEG) with glyoxal as crosslinking agent. They reported the feasibility of both injection and hot press molding to obtain standard samples for characterization (Selling et al., 2009).

Wang *et al.* (Wang and Padua, 2003), interestingly reported manufacturing of zein films plasticized with oleic acid (approx. 41.1 wt.%), by extrusion-blow molding, showing the feasibility of this process at industrial scale. Chen *et al.* (Chen et al., 2013), developed zein-based films, containing glycerol and polypropylene carbonate (PPC), by direct extrusion in a twin-screw extruder with a special dye.

Zein has been used as an additive (up to 20 wt.%) of thermoplastic starch to provide improved water resistance due to the hydrophobic nature of zein protein as reported by Grissel Trujillo-de Santiago *et al.* (Trujillo-de Santiago et al., 2014). In a similar way, Lim *et al.* (Lim and Jane, 1994), developed starch-zein plastics by injection molding using glycerol and water as plasticizers. They also studied the effect of the storage conditions (relative humidity), on final properties, concluding the positive effect of high relative humidity on mechanical properties since moisture can contribute to plasticize injection molded samples. On the other hand, thermoplastic zein materials have been successfully obtained by blending with polyvinyl pyrrolidone (PVP) of different molecular weight. PVP is compatible with zein and leads to good thermoplasticization with up to 20 wt.% PVP (Sessa et al., 2011). Selling (Selling, 2010), confirmed exceptional processing of plasticized zein by extrusion with water and triethyl citrate (TEC), and concluded extrusion temperature in the 100 – 140 ºC leads to optimum mechanical properties. Di Maio *et al.*

(Di Maio et al., 2010), reported thermoplastic zein materials by using 25 wt.% different plasticizers such as lactic acid, stearic acid or polyethylene glycol (PEG), and lauric acid. These materials were processed by twin counter-rotating internal mixer equipped with roller rotors, and subsequent thermocompression. Oliviero *et al.* (Oliviero et al., 2010), also reported the feasibility of obtaining thermoplastic zein films by blow-molding process using polyethylene glycol as plasticizer (25 wt.%).

Recently Alsadat-Seyedbokaei *et al.* (Alsadat-Seyedbokaei et al., 2023; Alsadat-Seyedbokaei et al., 2024), have reported the development of recyclable protein-based thermoplastics (zein and soy protein isolate) processed by injection molding. Previous mixing was carried out in a two blade counter-rotating rheometer which slightly differ from extrusion with twin-screw extruder, leading to lower tensile strength values. Regarding zein-based materials, they observed a glycerol to zein ratio of 25/75 gave the best-balanced properties, as well as recyclability. Processing by injection molding can be carried out at moderate temperatures of 150 ºC since they observed a clear softening above 80 ºC. Bouman *et al.* (Bouman et al., 2015), evaluated the potential of zein as matrix for controlled drug delivery. They prepared injection molded caplets with different paracetamol loadings to assess the delivery rate. Despite there is a lot of literature on thermoplastic zein manufactured by the cast film process, there are not as many studies on processing by extrusion, and even fewer studies on injection molding. Moreover, although there have been numerous investigations with thermoplastic zein using various plasticisers, glycerol remains one of the most appropriate plasticizers for zein, and no systematic study of the effect of glycerol content on extrusion/injection processing and overall properties of these materials has been done.

This works deals with an in-depth study of the effects of the plasticizer (glycerol) loading on mechanical, thermal, thermomechanical, wetting properties, and surface appearance of thermoplastic zein (TPZ), processed by extrusion and subsequent injection molding, thus showing the feasibility of these industrial scalable up processes as an environmentally friendly alternative to petroleum-derived commodity plastics.

2. Experimental.

2.1. Materials.

Zein (CAS number: 9010-66-6), was purchased form Sigma-Aldrich (Madrid, Spain) as a yellow to very dark yellow powder. Its moisture is equal or less than 8%. Glycerol (CAS number: 56-81-5), ACS reagent grade (>99.5%) from Sigma-Aldrich Spain (Madrid, Spain), was used without further purification.

2.2. Manufacturing of plasticized zein formulations by extrusion/injection molding.

Zein powder underwent initial heating at 80 ºC for 12 hours to eliminate residual moisture. Subsequently, the zein powder was mixed with different weight percentages of glycerol ranging from 15% to 40%, then were pre-blended in aluminum pods and introduced into a 15-cc twin-screw micro compounder Xplore MC 15 HT from Xplore Instruments BV (Sittard, The Netherlands). All zein-based formulations were mixed at a temperature of 130 ºC for 2 minutes, employing a screw speed of 100 rpm. Following this, the heated blends were introduced into the detachable barrel of a 12-cc micro injection molding machine Xplore IM 12 from Xplore Instruments BV (Sittard, The Netherlands) and injected into a mold cavity using a plunger to produce standard samples. The injection molding process was conducted at 135 ºC. Post-demolding, the samples were preserved in a vacuum desiccator at room temperature for subsequent characterization. Samples were stored in a vacuum desiccator at a relative humidity of 53%, at room temperature for 1 week for further characterization.

2.3. Mechanical properties.

The tensile properties of thermoplastic zein formulations, incorporating varying quantities of glycerol, were assessed using a universal testing machine, namely the IBERTEST DUOTRAC 10/1200 model from S.A.E. Ibertest (Madrid, Spain), equipped with a 10 kN load cell in accordance with ISO 527-2:2012. The testing protocol involved setting the crosshead speed at 5 mm min^{-1} and the initial length at 50 mm to facilitate accurate calculation of the elongation at break. Specifically, the elastic modulus (E), the maximum tensile strength (σ_{max}), and

percentage elongation at break (%ε_b) were determined for a minimum of five distinct samples, and the resultant average values, alongside standard deviations, were derived. Furthermore, the work of fracture (WOF) was computed by integrating the area under the stress-strain curve and averaged across at least five distinct samples.

The impact strength assessment for thermoplastic zein formulations containing glycerol was conducted utilizing unnotched samples subjected to a Charpy impact pendulum (1-J) from Metrotec S.A. (San Sebastian, Spain), in accordance with ISO 179 standards.

Shore D hardness evaluations for thermoplastic zein formulations were conducted using a durometer, model 673-D from J. Bot S.A. (Barcelona, Spain), following the guidelines outlined in ISO 868:2003. A minimum of ten measurements were undertaken, and the average Shore D values, along with standard deviations, were determined for zein-based formulation.

2.4. Thermal and thermomechanical characterization.

The glass transition temperature (T_g) of thermoplastic zein formulations incorporating glycerol were investigated by differential scanning calorimetry (DSC) in a DSC-821 calorimeter from Mettler-Toledo Inc. (Schwerzenbach, Switzerland) under a nitrogen atmosphere (50 mL min^{-1}). Samples within the 5–10 mg range underwent a heating cycle from -50 to 250 ºC at a rate of 10 ºC min^{-1}. The thermal degradation of thermoplastic zein formulations, featuring varying glycerol content, was monitored through thermogravimetric analysis (TGA) employing a TG-DSC2 thermobalance from Mettler Toledo (Columbus, Ohio, USA). Samples weighing between 7 and 10 mg were placed into standard alumina cylindrical crucibles of 70 µL, covered with lids, and subjected to a dynamic heating program from 25 ºC to 700 ºC under a nitrogen atmosphere (50 mL min^{-1}) at a heating rate of 20 ºC min^{-1}. The first derivative TGA curve or DTG was plotted and the main thermal parameters regarding thermal degradation were obtained. All DSC and TGA characterizations were conducted in triplicate to ensure result reliability. Dynamic mechanical thermal analysis (DMTA) was executed using a Mettler Toledo DMA1 instrument (Columbus, Ohio, USA) operating under single cantilever conditions. The chosen frequency for the analysis

was set at 1 Hz, and the maximum amplitude in the free cantilever was established at 10 μm. Specimens measuring 25×10×4 mm³ on average were subjected to a dynamic heating ramp spanning from -50 ºC to 125 ºC with a heating rate of 2 ºC min^{-1}. The temperature-dependent evolution of the storage modulus (E') was collected.

2.5. Characterization of the zein-glycerol interactions.

The thermoplastic zein samples featuring increasing glycerol content underwent analysis through attenuated total reflectance Fourier transform infrared spectroscopy (ATR-FTIR) employing a Perkin-Elmer BX infrared spectrometer obtained from Perkin Elmer Spain, S.L. (Madrid, Spain). Prior to sampling, a background measurement was conducted within the wavenumber range of 4000-600 cm^{-1} to compensate for the environmental influences of moisture and carbon dioxide. FTIR-ATR spectra for all thermoplastic zein formulations were acquired as the average of 20 scans with a resolution of 4 cm^{-1}.

2.6. Contact angle and surface appearance.

Color measurements were conducted employing a Konica CM-3600d Colorflex-DIFF2 spectrophotometer sourced from Hunter Associates Laboratory, Inc. (Reston, VA, USA). The CIELab* color space coordinates were determined, where L* denotes luminance, a* signifies the color coordinate ranging from green (a* < 0) to red (a* > 0), and b* represents the color coordinate spanning from blue (b* < 0) to yellow (b* > 0). The color differences of samples with increasing glycerol content (sub index 2) (ΔE) with respect to the sample containing the lowest glycerol percentage in this study (sub index 1) was calculated following **Equation 1** (Comission Internationale de l'Eclaraige, 1977).

$$\Delta E = \sqrt{(L_2^* - L_1^*)^2 + (a_2^* - a_1^*)^2 + (b_2^* - b_1^*)^2} \qquad \textbf{Equation 1}$$

A minimum of 10 distinct measurements were performed on planar specimens, and the resultant average color coordinates were derived for analysis.

Surface wetting characteristics were assessed utilizing an optical goniometer, specifically the EasyDrop Standard model FM140 manufactured by KRÜSS GmbH (Hamburg, Germany),

which was augmented with a video capture accessory kit. Contact angle measurements were performed employing double distilled water and the Drop Shape Analysis SW21; DSA1 software. Flat specimens, measuring 80×10×4 mm^3, were employed to determine the water contact angle (θ_w) at room temperature. A minimum of 10 distinct measurements were conducted, and the resulting θ_w values were subjected to averaging for analysis.

2.7. Fracture surface morphology by field emission scanning electron microscopy (FESEM).

Examination of the fractured samples from impact test, as well as the supplied zein powder, was carried out by field emission electron microscopy (FESEM) on a ZEISS ULTRA 55 FESEM instrument sourced from Oxford Instruments (Abingdon, UK). The FESEM operation featured a set working distance ranging from 5 to 7 mm, and the electron beam acceleration voltage was fixed at 1.5 kV. Prior to microscopic observation, the fracture surfaces underwent a sputtering treatment with a gold-palladium alloy, conducted using a SC7620 sputter coater manufactured by Quorum Technologies Ltd. (East Sussex, UK).

3. Results and discussion.

3.1. Effect of glycerol on chemical interactions and mechanical properties of plasticized zein.

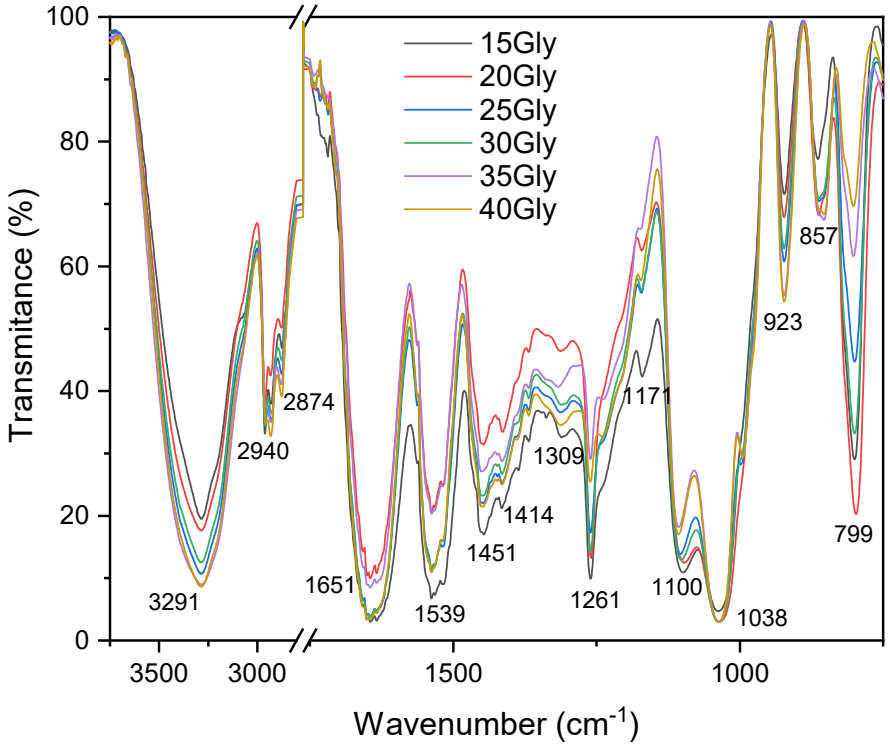

Figure 1. Fourier transform infrared spectra (FTIR) of thermoplastic zein with different amounts of glycerol.

Figure 1 gathers a comparative plot of the FTIR spectra of TPZ with different amounts of glycerol. Proteins usually show nine absorption bands identified as amide I-VII, A, and B (Jiang et al., 2023a), but the most important peaks that can be seen are the amide A, I, II and III bands. The A band comprises different peaks comprised between 3600 – 3100 cm^{-1}. The wide band cantered at 3280 cm^{-1}, corresponds to the stretching vibration of O–H groups. As it can be seen in **Figure 1**, as the glycerol content increases the area of this peak also increases due to the extra O–H groups provided by glycerol. The amide I is the most intense absorption band in proteins. It can be detected by a region located between 1600 and 1800 cm^{-1}, and corresponds to C=O stretching vibrations and, in a less extend to N–H vibrations (Barth, 2007). This band is widely used to assess the secondary structure of proteins. As it can be seen in **Figure 1**, different amide I vibrations can be seen as small peaks in this region. As this is a characteristic peak of the zein protein, it shows

the maximum intensity in TPZ with the lowest glycerol content (15 wt.%), as expected. The amide II typical absorption band is located between 1510 – 1580 cm^{-1}. This mainly corresponds to in-plane N–H bending and, in a less extend, to C–N, and C–C stretching vibrations (Mattice and Marangoni, 2020). This region is highly affected by the presence of glycerol. The main intensity corresponds to TPZ with 15 wt.%, and, as the zein content decreases (more plasticized materials), the intensity of this peak also does. Finally, the amide III band has a range comprised between 1350 – 1200 cm^{-1} and, despite it shows a weaker signal compared to amide I and amide II, it provides information about the protein secondary structure (Cai and Singh, 1999, 2004). The amide III region is related to the in-phase combination of N–H in-plane bending, and C–N stretching vibrations (Cai and Singh, 2004). The wavenumber range comprised between 1480 – 1200 cm^{-1}, has been proposed as the dactylogram of proteins. This region is associated to amide structure tautomerism and single bond vibration of C–H, and N–H. Once again, the most intense signal in this region corresponds to the TPZ with 15 wt.% glycerol and less intensity is observed with increasing the glycerol content. The effect of glycerol on FTIR spectra of TPZ can also be observed through the peak located at 1038 cm^{-1}, which corresponds to the O–H deformation vibration. This peak has increased intensity as the glycerol content increases.

Molecular dynamics (MD) simulation has proven to be an efficient technique to predict the mechanical properties of well-defined thermoplastic starch from amylose (Özeren et al., 2020), or amylopectin (Mojica-Munoz et al., 2024). Nevertheless, in the case of proteins, their chemical structure is more complex due to the primary, secondary, and higher structure levels, as well as the denaturation process provided by the plasticizer and/or temperature. Despite Özeren *et al.* (Özeren et al., 2021) have reported the usefulness of molecular dynamics simulations in elucidating the plasticization mechanisms in a gluten/glycerol/water system (20-30 wt.%), they only considered low molecular weight glutenin (well-known chemical structure) as the base polymer. Anyway, the results obtained by MD are very promising in designing new efficient plasticizer molecules for polymers. A macroscopic study of the efficiency of a plasticizer can be carried out by measuring its effect son mechanical, thermal and thermomechanical properties.

The effect of glycerol can also be observed in mechanical properties of TPZ with different glycerol content as shown in **Figure 2**, which gathers the comparative stress-strain tensile curves for of TPZ developed in this study. As can be seen, samples with 15, 20, and 25 wt.% show higher tensile strength and elongation at break than TPZ materials with higher glycerol content (30 wt.% and above). This suggests that addition of glycerol provides interesting plasticization at glycerol contents between 15 – 25 wt.%. Compositions with lower glycerol content (<5 wt.%) can not be processed by extrusion and injection molding. On the other hand, despite it is possible to obtain TPZ by extrusion and injection molding with high glycerol content, the obtained TPZ materials are more brittle which could restrict their use. **Table 1** summarizes the main mechanical properties of TPZ with different glycerol content, obtained from standard tensile, hardness and impact tests. It is worthy to note that the tensile strength of TPZ with 15 wt.% glycerol is comparable to some commodities, with a value of 27.9 MPa, and a modulus of 785 MPa. The elongation at break (%ε_b) is 5.2%. As the glycerol content increases, the plasticization effects on mechanical properties can be clearly seen. The maximum tensile strength (σ_{max}), and the modulus, decrease progressively with the glycerol content down to values of 5.0 MPa, and 218 MPa, respectively for the TPZ containing 40 wt.% glycerol. Nevertheless, the elongation at break, which gives information of the material's toughness, increases to 6.4% for the TPZ with 20 wt.% glycerol, and decreases down to values below 3.8% in TPZ formulations containing 30 wt.% glycerol, and above. These results are very promising since these materials could play a key role in substitution of some commodity plastics. These results are in agreement with those reported by Chen *et al.* (Chen et al., 2013), in zein/glycerol films containing different amounts of polypropylene carbonate (PPC). They reported a tensile strength of 20-24 MPa for TPZ with different zein:glycerol ratios (10:1; 10:2, and 10:3) and 15% PPC, while the elongation at break of these materials was comprised between 2.0-2.5%.

As reported in literature, zein contains many hydrogen bonds among the hydroxypropyl groups since this protein contains serin and threonine amino acids as reported by Biswas *et al.* (Biswas et al., 2009). When zein is mixed with glycerol, glycerol molecules locate between polymer chains thus reducing the intensity of these hydrogen bonding which results in a decrease

in tensile strength, in accordance with a decrease in the glass transition temperature, Tg as observed by molecular dynamics simulations in plasticized gluten with glycerol (Özeren et al., 2021). The decrease in Tg will be discussed in the next section, but this decreases from 42.3 ºC (15 wt.% glycerol) down to 36 ºC (35 wt.% glycerol) gives support to the decrease in tensile strength due to weakening the hydrogen bonding provided by glycerol. This same behavior has been observed by Wongsasulak *et al.* (Wongsasulak et al., 2010) in plasticized zein electrospun films. On the other hand, glycerol also exerts a plasticization effect, enhancing the flexibility and polymer chain mobility due to a lubrication effect. Nevertheless, an excess plasticizer leads to a loss in the matrix cohesion, thus leading to a sticky state with low cohesion, as observed in high glycerol content zein blends. This behavior has been observed by Sánchez *et al.* (Sánchez et al., 1998), who reported this lack of cohesion in plasticized gliadin films with 28.1 wt.% glycerol and additional 9.0 wt.% water.

Alsadat-Seyedbokaei *et al.* (Alsadat-Seyedbokaei et al., 2023), have reported similar the effect of different glycerol content and processing temperature on mechanical properties of TPZ materials. The modulus of zein/glycerol materials with 25-35 wt.% glycerol is similar to the results we obtained. Nevertheless, they reported lower tensile strength (σ_{max}), and elongation at break ($\%\varepsilon_b$), less than 3.54 MPa, and 1.5% for all materials, thus suggesting, the processing conditions have a remarkable effect on mechanical properties. Wang *et al.* (Wang and Padua, 2003), also reported lower tensile strength values of 3-4 MPa while they observed a high elongation at break of 100-120% depending on the extrusion process (single-screw or twin-screw extrusion). Lim *et al.* (Lim and Jane, 1994), obtained similar results in starch/zein materials with tensile strength values comprised between 20-25 MPa, and elongation at break values of 3.5-4.7%. They also reported the effect of the drying conditions on mechanical properties, since storage at low relative humidity leads to embrittlement.

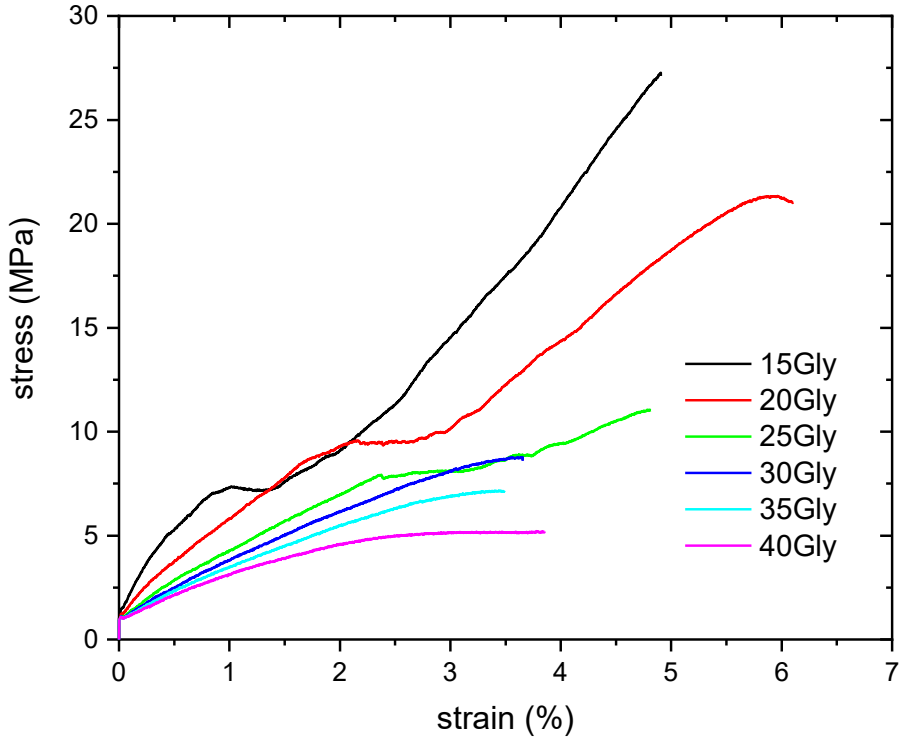

Figure 2. Comparative plot of the stress-strain (σ-ε) tensile plots of thermoplastic zein with different plasticizer amounts.

Table 1. Summary of the mechanical properties of thermoplastic zein with different plasticizer amounts.

wt.% glycerol	Tensile strength, σ_{max} (MPa)	Young's modulus, E (MPa)	Elongation at break, ε_b (%)	Work of fracture (MJ m^{-3})	Impact strength (kJ m^{-2})	Shore D hardness
15	27.9 ± 0.8	785 ± 24	5.2 ± 0.1	63.6	5.1 ± 0.1	75 ± 1
20	20.6 ± 0.5	534 ± 39	6.4 ± 0.4	72.1	6.6 ± 1.1	69 ± 1
25	11.2 ± 0.5	386 ± 19	5.0 ± 0.1	33.2	8.0 ± 1.4	61 ± 1
30	8.5 ± 0.6	309 ± 22	3.8 ± 0.5	20.2	9.0 ± 2.1	58 ± 1
35	7.2 ± 0.5	279 ± 23	3.1 ± 0.5	16.5	9.3 ± 1.6	52 ± 1
40	5.0 ± 0.1	218 ± 14	3.0 ± 0.7	15.3	8.7 ± 1.1	49 ± 1

The tensile toughness of TPZ materials has been assessed by the calculation of the are under the stress-strain curve or work of fracture. As can be seen in **Table 1**, the TPZ with the highest tensile toughness is the formulation with 20 wt.% glycerol, with a value of 72.1 MJ m^{-3}. TPZ with 15 wt.%, and 25 wt.% glycerol, show a tensile toughness of 63.6, and 33.2 MJ m^{-3}. As expected from the stress-strain curves, TPZ formulations with 30 wt.% glycerol, and above, are more brittle which leads to lower tensile toughness values between 15 – 20 MJ m^{-3}. Anyway, these tensile toughness values are comparable to those reported by Liu *et al.* (Liu et al., 2019), in plasticized PLA with epoxidized soybean oil, with tensile toughness of 52.8 MJ m^{-3}. With regard to the Charpy's impact test as samples are subjected to impact conditions, the energy absorption is lower than that observed in a tensile test. The highest impact strength values are obtained for TPZ materials containing 30 – 40 wt.% glycerol, with values of around 9 kJ m^{-2}, while the impact strength of the composition containing 20 wt.% is 6.6 kJ m^{-2}. As expected, the Shore D harness decreases with increasing the glycerol content due to the plasticization effect glycerol provides to TPZ.

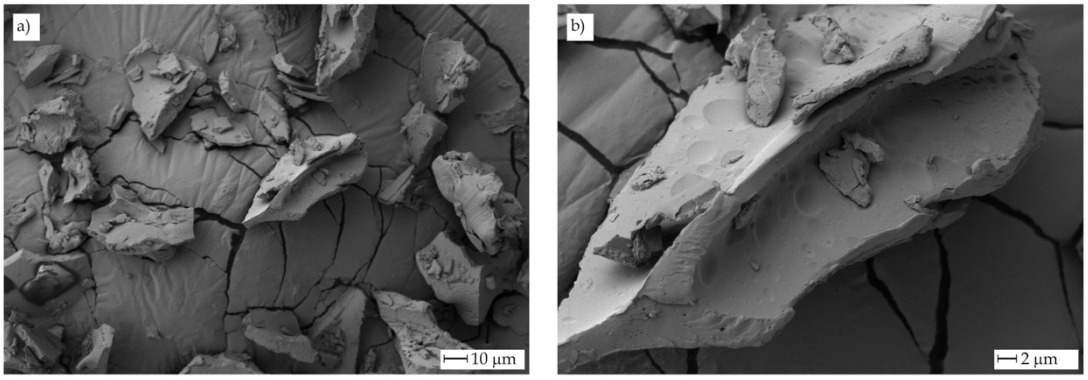

Figure 3. Field emission scanning electron microscopy (FESEM) images of the of zein powder particles at different magnifications a) 500×, scale bar = 10 µm, and b) 2000×, scale bar = 2 µm.

Figure 3 shows the morphology of the zein powder. Irregular shapes with a size of 20 µm×40 µm, can be observed. **Figure 4** shows the fracture surface morphology obtained from

fractured samples in Charpy's test. All samples exhibit spherical microvoids on the fracture surface. As the glycerol content increases, the presence of these microvoids intensifies.

Sessa *et al.* (Sessa et al., 2011), have reported the presence of these microvoids in plasticized zein blends with polyvinylpyrrolidone (PVP). These cavities were attributed to trapped bubbles. Similar SEM characteristics have been reported by Bouman *et al.* (Bouman et al., 2016), who observed pores in zein-based caplets for drug delivery. They attributed this to trapped air during mixing and proved that loaded drugs located preferentially in these pores. These cavities may appear as a consequence of the evaporation of the residual moisture or simply due to the mechanical mixing in the extruder.

These microvoids are responsible for the previously described low elongation at break values. In the sample containing 20 wt.% glycerol (**Figure 4b**), clear signs of plastic deformation are evident, with various areas of high roughness resulting from material stretching during the deformation and fracture process. These rough areas are also observed in TPZ samples with 25 wt.% glycerol (**Figure 4c**). Above 30 wt.% glycerol, the presence of spherical voids increases. These microvoids act as stress concentrators and negatively impact the material's toughness, as previously described. Fractures corresponding to TPZ samples with high glycerol content (**Figure 4e** and **Figure 4f)** exhibit a fracture surface with multiple microcracks and microvoids acting as stress concentrators, resulting in materials with low elongation at break.

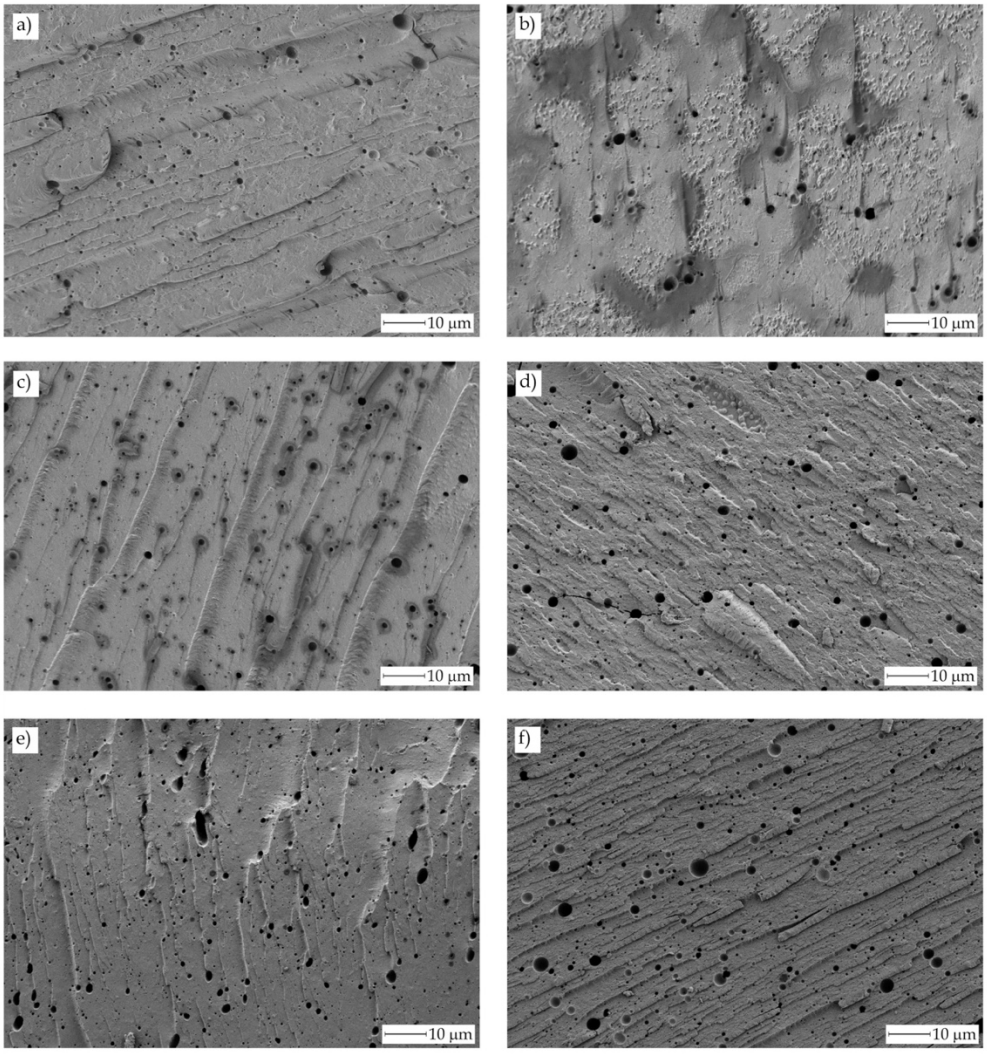

Figure 4. Morphology of fractured surface of thermoplastic zein with different amounts of glycerol (wt.%): a) 15, b) 20, c) 25, d) 30, e) 35, and f) 40. Scale bar XX µm).

3.2. Thermal and thermo-mechanical properties of thermoplastic zein with glycerol.

Figure 5 shows a comparative plot of the first heating cycle obtained by DSC. The glass transition temperature, T_g can be seen as the change in the slope in the 40 – 70 ºC range which is associated to a change in the heat capacity (C_p). It has been reported, unplasticized zein possesses a T_g in the 150 - 180 ºC, usually measured in the form of film obtained by solvent casting (Gillgren et al., 2009). It is virtually impossible to obtain TPZ by extrusion and injection molding without using a plasticizer. Plasticization with glycerol exerts an important effect on T_g. As it has been reported by Xu *et al.* (Xu et al., 2012), the hydrogen bonding of glycerol with zein increases the

available number of end groups and, subsequently, the free volume is increased too, this having an effect on decreasing the T_g values. Huo *et al.* (Huo et al., 2018), proposed that glycerol molecules promote a disruption of the α-helix packing, and an increase in the β-sheet content. Then, glycerol molecules place between β-sheets and, subsequently, the hydrogen bonding interactions between β-sheets decrease, thus leading to a plasticization effect. The TPZ with the lowest glycerol content able to be processed by injection molding, (15 wt.%) shows a T_g of about 42.3 ºC, which indicates good plasticization efficiency (**Table 2**). As the wt.% glycerol increases, a slight decrease in T_g can be observed down to values in the 36 – 38 ºC range for TPZ materials with 25 – 40 wt.% glycerol. These results agree to those of Lawton (Lawton, 2004), who observed that glycerol content above 20 wt.% did not provide significant changes in T_g (with values around 50 ºC), of plasticized zein cast films, while other plasticizers such as triethylene glycol (TEG) did provide a decreasing tendency on T_g as the TEG content increased. Almeida *et al.* (de Almeida et al., 2018), reported slightly higher T_g values (comprised between 47 – 49 ºC) on plasticized zein films containing approximately 41.2 wt.% of different plasticizers, namely buriti, olive and macadamia oils, thus confirming that large amounts of some plasticizers do not give a remarkable decrease in T_g above certain threshold.

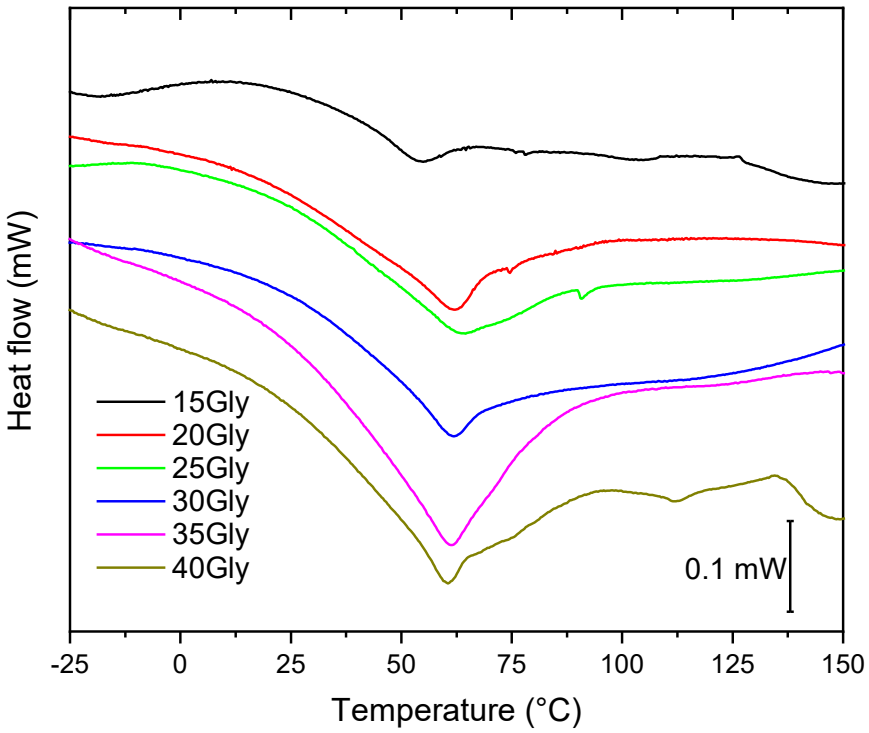

Figure 5. Comparative plot of the differential scanning calorimetry (DSC) plots of thermoplastic zein with different plasticizer amounts.

Table 2. Glass transition temperature (T_g) of thermoplastic zein with different amounts of glycerol, obtained by differential scanning calorimetry (DSC).

wt.% glycerol	**Glass transition temperature, T_g (°C)**
15	42.3 ± 2.1
20	40.9 ± 2.5
25	38.3 ± 1.9
30	37.9 ± 2.6
35	36.3 ± 2.5
40	37.8 ± 1.9

Figure 6a shows a comparative plot of the thermogravimetric (TGA) curves for TPZ with different glycerol content. As expected, the mass loss occurs in two clearly differentiated processes (Cao et al., 2023; Xu et al., 2023). Additionally, a third process is noticeable at temperatures around 100 ºC, corresponding to the removal of residual water (Oliviero et al., 2010). The first highlighted mass loss process occurs between 150 – 270 ºC, corresponding to the loss of the plasticizer, glycerol, as it has a lower molecular weight structure than zein and degrades at lower temperatures (Almazrouei et al., 2022). The zein degradation process occurs between 250 – 450 ºC, resulting in an ash residue that increases with higher zein content. Han *et al.* (Han et al., 2023), have shown that the degradation of unplasticized zein occurs in a single stage between 250 – 450 ºC, with a degradation peak temperature around 225 – 230 ºC and a residual mass of 17.66%. In the enlarged graph of **Figure 6a**, the glycerol loss process is clearly distinguished. **Table 3** shows the mass loss in this initial step for different TPZ formulations. The mass loss correlates completely with the glycerol content in TPZ. In particular, the mass lost in this initial step is slightly higher than the nominal glycerol amount in different TPZ formulations, as besides glycerol loss, the zein degradation also initiates (Oliviero et al., 2010). The analysis of the 1st derivative (DTG) of the thermogravimetric curves provides relevant information (**Figure 6b**). The two indicated processes are clearly distinguished, with two peaks showing overlap around 270 ºC, thus confirming the mass loss results in the process attributed to glycerol removal. The peak corresponding to the maximum degradation rate in the first process, T_{max1} (glycerol loss), shifts from 261 ºC (15 wt.% glycerol) to lower values of 241 ºC (40 wt.% glycerol). This phenomenon suggests that the interactions between glycerol and zein are more intense for low glycerol amounts, providing a thermal stabilization effect. As the glycerol content increases, the interaction with zein does not significantly improve, as previously observed in the characterization of T_g using DSC, leading to easier removal and reduced T_{max1} values. Regarding the second mass loss process in the range of 280 – 450 ºC, corresponding to zein degradation, the temperature of the maximum degradation rate (T_{max2}) remains almost constant, ranging between 321 – 326 ºC, and aligns with values reported by Han *et al.* (Han et al., 2023), for unplasticized zein.

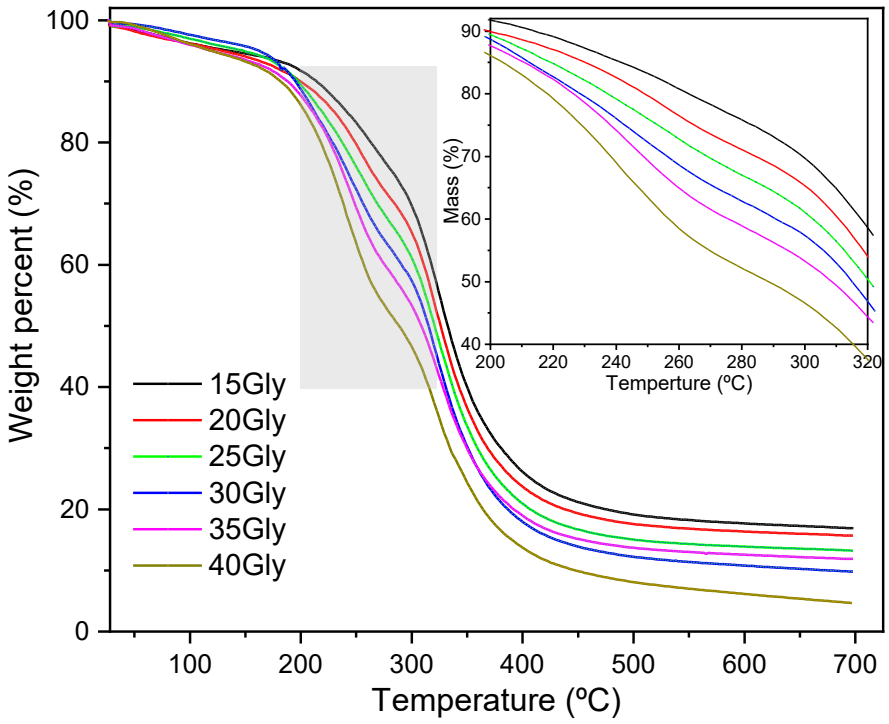
Weight percent (%)
Temperature (ºC)
15Gly
20Gly
25Gly
30Gly
35Gly
40Gly
Mass (%)
Temperture (ºC)

a)

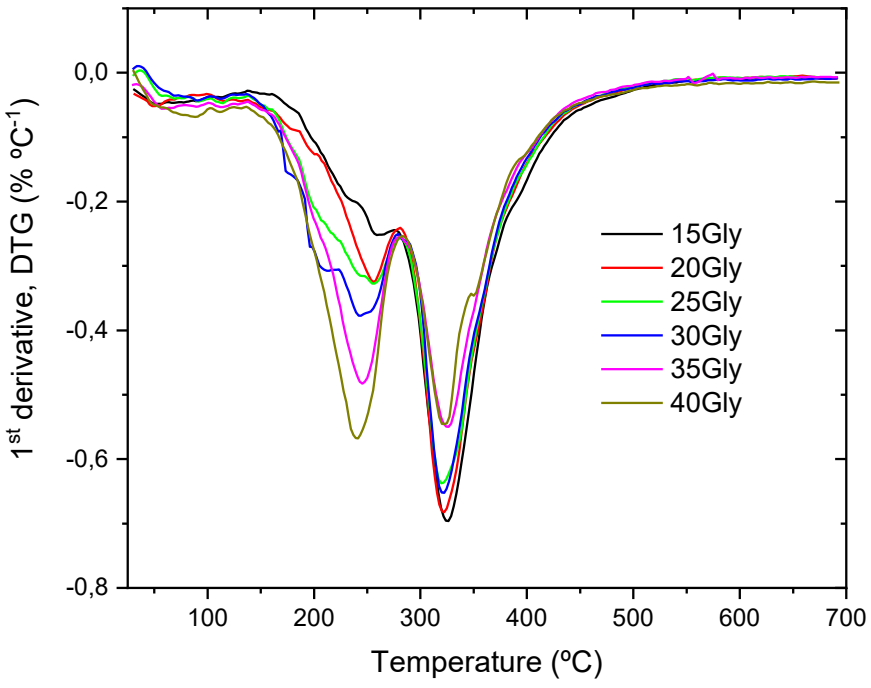
1st derivative, DTG (% ºC-1)
Temperature (ºC)
15Gly
20Gly
25Gly
30Gly
35Gly
40Gly

b)

Figure 6. Plots of the thermogravimetric (TGA) degradation curves of thermoplastic zein with different amounts of glycerol, a) mass loss vs temperature, and b) first derivative DTG.

Table 3. Main parameters regarding the thermal degradation of thermoplastic zein with different amounts of glycerol.

wt.% glycerol	Mass loss step 1 (%)	T_{max1} (ºC)	T_{max2} (ºC)	Residual mass
15	20.2 ± 0.3	261 ± 3	326 ± 3	16.9 ± 0.3
20	24.4 ± 0.3	256 ± 2	323 ± 2	15.7 ± 0.2
25	29.5 ± 0.4	254 ± 2	321 ± 3	13.2 ± 0.4
30	34.3 ± 0.2	241 ± 3	321 ± 2	9.8 ± 0.5
35	37.1 ± 0.4	243 ± 2	324 ± 3	12.0 ± 0.2
40	43.4 ± 0.5	241 ± 2	321 ± 2	4.7 ± 0.1

In relation to the mechanical-dynamic behavior, **Figure 7** shows a comparison of the evolution of the storage modulus (E') as a function of temperature for TPZ with different glycerol contents. As the glycerol content increases, a shift of the DMTA curves towards lower storage modulus values is observed. At room temperature, the storage modulus for TPZ with 15 wt.% glycerol is 1050 MPa. This value reduces to 620 MPa for TPZ with 20 – 25 wt.% glycerol and further to 390 MPa for glycerol contents of 35 – 40 wt.%. The softening process associated with the glass transition is clearly distinguished in the temperature range between 50 – 70 ºC, coinciding with values described previously in the section corresponding to the study using differential scanning calorimetry (DSC). Above T_g, the storage modulus, E' values decrease by about 2 – 3 orders of magnitude, providing clear evidence of softening. Alsadat-Seyedbokaei *et al.* (Alsadat-Seyedbokaei et al., 2023), have reported similar results for zein plasticized with different glycerol contents, processed by extrusion and injection molding at different temperatures. These results are also consistent with those reported by Ghanbarzadeh *et al.* (Ghanbarzadeh and Oromiehi, 2009), in plasticized zein with glycerol, with slightly higher T_g

values above 60 ºC. Corradini *et al.* (Corradini et al., 2006), demonstrated the plasticizing effect of glycerol in zein films. In particular, they observed that up to 22% glycerol content, the T_g decreased to 63 ºC, and for higher glycerol amounts, there were no significant changes in T_g. In any case, the T_g values obtained by DMTA were always higher than those obtained by DSC.

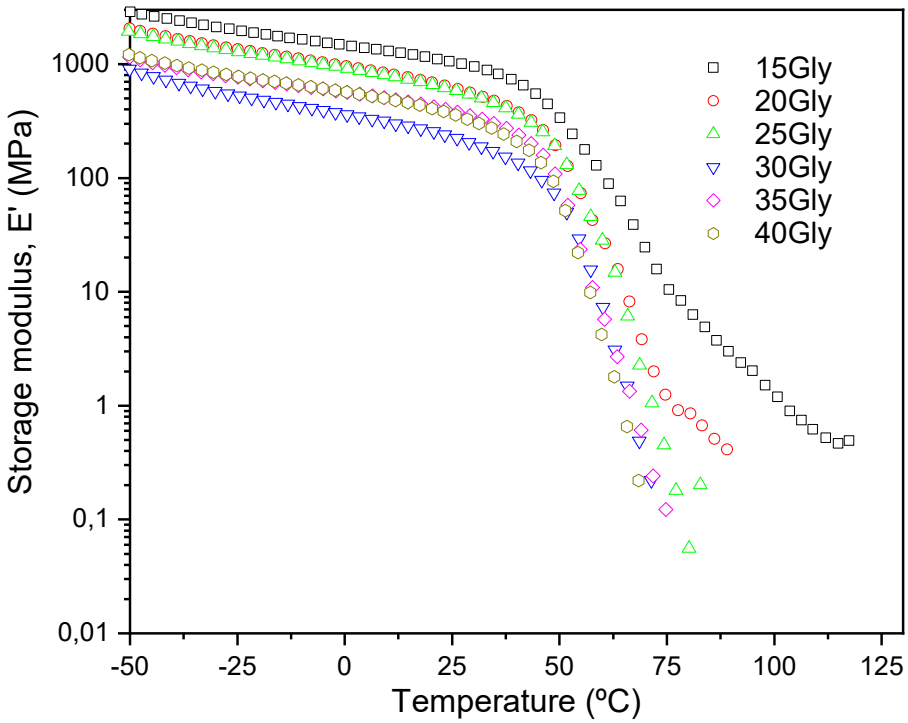

Figure 7. Comparison plots of the storage modulus (E') versus temperature of thermoplastic zein with different amounts of glycerol, obtained by dynamic-mechanical thermal analysis (DMTA).

3.3. Colour and wetting properties of plasticized zein with glycerol.

Figure 8 presents a comparative image of the appearance of TPZ samples with different glycerol content, obtained through extrusion and subsequent injection molding. All TPZ samples exhibit a good surface finish and excellent shape reproducibility, demonstrating the feasibility of the injection molding process for producing TPZ parts. Regarding color, TPZ samples with low glycerol content (between 15 and 25 wt.%) have a subdued brown hue. However, TPZ samples with high glycerol content (30 – 40 wt.%) display a more reddish-orange tint. Quantification of color changes was carried out by measuring the colorimetric coordinates L*, a*, b* (**Table 4**). In

terms of brightness, L*, all developed TPZ samples have fairly similar values, ranging between 31 – 36. Concerning the color coordinate a*, which indicates the color content between green (a*<0) and red (a*>0), samples with low glycerol content have low a* values, ranging between 1.30 and 1.58. As qualitatively observed, samples with higher glycerol content (30 – 40 wt.%) exhibit a more pronounced reddish hue, quantifiable by higher a* values ranging between 3.57 and 6.80. Regarding the color coordinate b*, representing color content between blue (b*<0) and yellow (b*>0), a similar behavior is observed based on glycerol content. In samples with low glycerol content (15 – 25 wt.%), the b* coordinate is positive (yellow), reaching values between 10 – 11, while samples with higher glycerol content exhibit a more intense yellow hue (b* between 10 and 15), resulting in reddish-orange tones. The color variation (ΔE) has also been determined, and as expected, it increases with glycerol content.

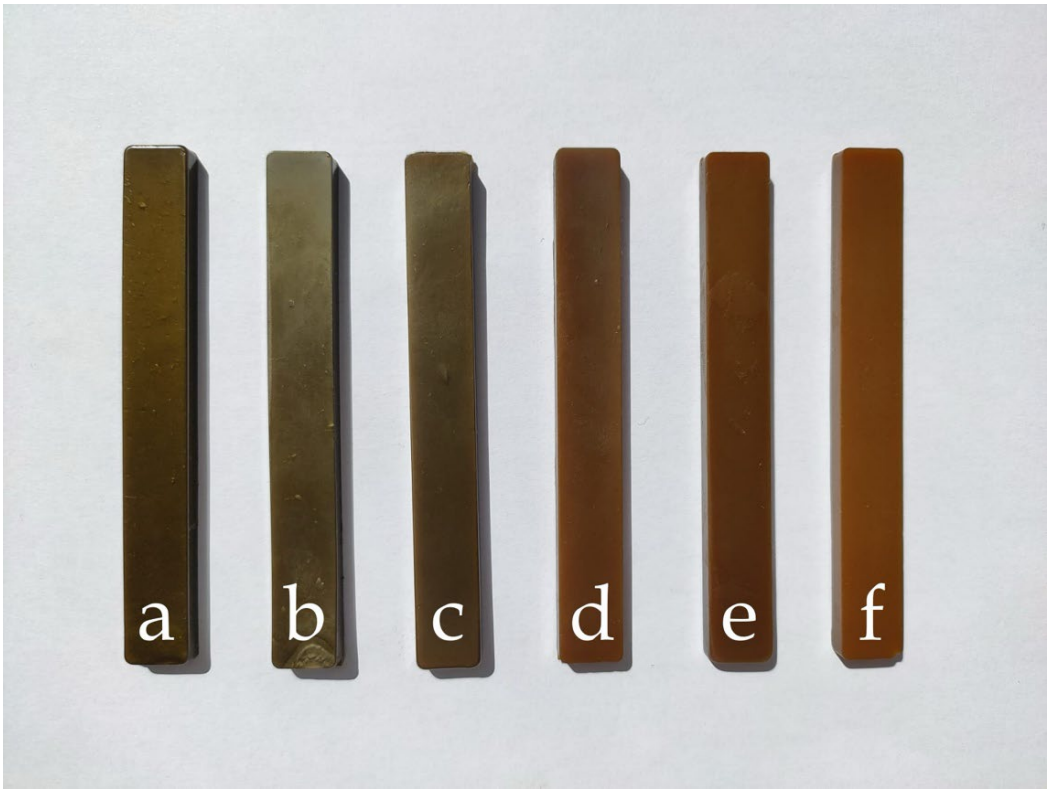

Figure 8. Visual appearance of injection molded thermoplastic zein samples with different amounts of glycerol.

Table 4. Color indexes (L*, a*, b*) of injection molded thermoplastic zein samples.

wt.% glycerol	L*	a*	b*	ΔE
15	35.14 ± 0.60	1.58 ± 0.31	11.58 ± 0.71	-
20	36.21 ± 0.16	0.65 ± 0.09	10.70 ± 0.14	1.67
25	34.68 ± 0.57	1.30 ± 0.15	10.07 ± 0.26	1.77
30	32.72 ± 0.63	3.57 ± 0.14	10.31 ± 0.50	3.38
35	31.04 ± 0.56	4.49 ± 0.33	12.20 ± 1.14	5.07
40	33.72 ± 1.21	6.80 ± 0.38	15.50 ± 1.10	6.67

Regarding surface wettability properties, **Figure 9** displays the water contact angle of TPZ with different glycerol content. While zein is a protein with a high hydrophobic nature, the incorporation of glycerol has a very clear and evident effect on wettability. TPZ with low glycerol content exhibits the highest hydrophobicity, with a water contact angle of 54.1°, whereas the TPZ sample with higher glycerol content demonstrates greater wettability. Its inherent hydrophilic nature is intensified by the presence of higher glycerol content, reaching a contact angle of 32.2°. Shi *et al.* (Shi et al., 2009), demonstrated that the water contact angle in zein films depends on the solvent used in the casting process, as it can affect the secondary and tertiary structure of zein. They concluded that the water contact angle of zein films obtained in an aqueous solution with acetic acid (60 – 90%), practically did not alter the contact angle, with a value around 75 – 80°. However, when using ethanol, the contact angle was very sensitive to the ethanol proportion in the solution used for film formation, ranging between 40° - 70° for ethanol percentages of 60 to 95% in aqueous solution. Chen *et al.* (Chen et al., 2014), also observed this effect in zein films obtained with aqueous solutions of ethanol and isopropanol in different proportions. Ghanbarzadeh *et al.* (Ghanbarzadeh et al., 2006), demonstrated the effect of different polyols on the water contact angle of plasticized zein films. Unplasticized zein films presented a contact

angle of 62.3°, while films plasticized with glycerol offered a contact angle of 52.48°, with glycerol contents of approximately 30%, which are in accordance to the herein reported values.

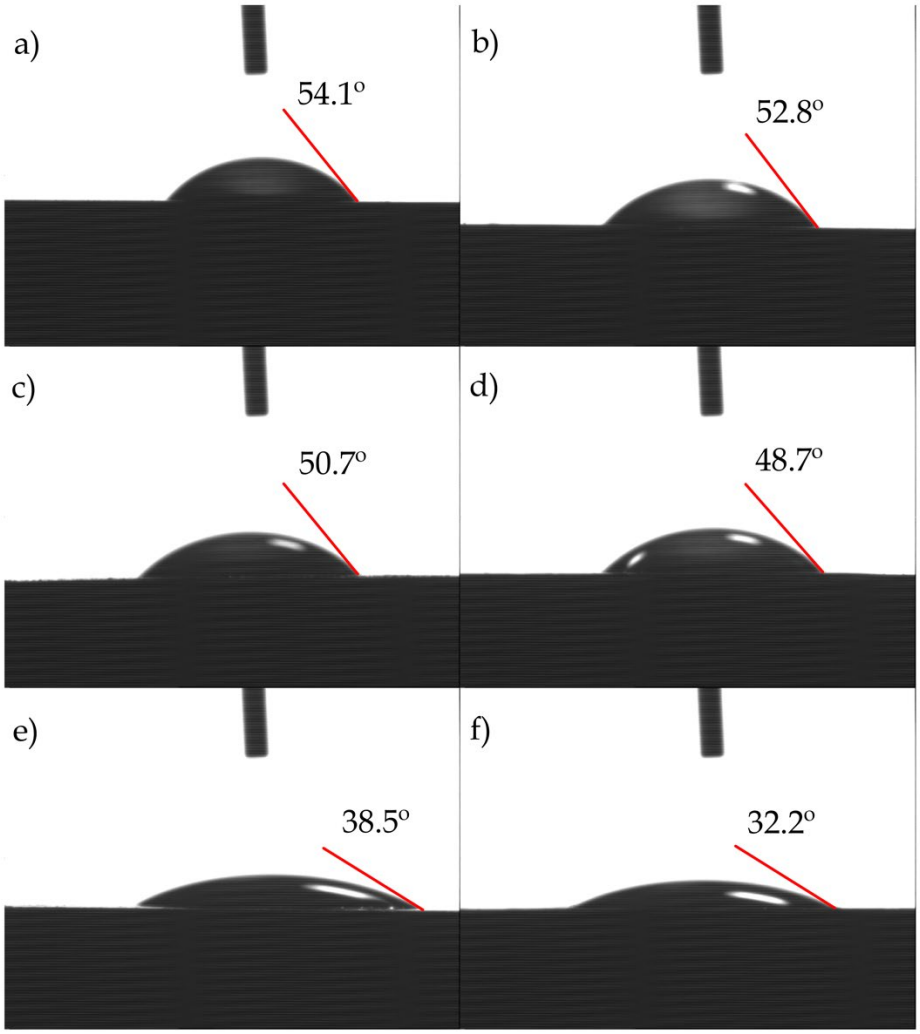

Figure 9. Comparison of surface wettability of thermoplastic zein with different amounts of glycerol obtained by static water contact angle.

4. Conclusions.

This research demonstrates the feasibility of extrusion and injection molding processes to obtain thermoplastic zein (TPZ). The use of a plasticizer is necessary to process these materials using these techniques. A minimum of 15 wt.% glycerol is required to properly process the materials, while for plasticizer contents exceeding 40 wt.%, heterogeneous mixtures are achieved, as the material expels the excess plasticizer. The mechanical properties of the obtained TPZ are

interesting for a glycerol content between 15-25 wt.%, with tensile strength values ranging from 11.0-27.9 MPa and elongation at break values of 5.0-6.4%. Compositions with higher glycerol content (>25 wt.%) exhibit very poor mechanical properties and increased fragility due to the presence of microvoids in the material structure. The glass transition temperature is reduced to values around 40 ºC, demonstrating the effectiveness of glycerol as a plasticizer. The degradation of these materials occurs in two stages, as shown by thermogravimetric analysis. Glycerol loss occurs between 150-270 ºC, and protein degradation occurs in the temperature range between 250-450 ºC. Glycerol-plasticized TPZ materials exhibit a brownish hue that shifts towards more reddish-orange colors as glycerol content increases. As expected, with the increase in glycerol content, the water contact angle, representative of hydrophilicity, significantly decreases from 54.1º (15 wt.% glycerol) to 32.2º (40 wt.% glycerol). These processing techniques offer new technological possibilities for zein, establishing the groundwork for its industrial-scale processing through extrusion and injection molding, expanding the potential of these materials in replacing petroleum-derived commodity plastics.

Acknowledgements.

This research is a part of the grant PID2020-116496RB-C22, funded by MCIN/AEI/10.13039/501100011033 and the grant TED2021-131762A-I00, funded by MCIN/AEI/10.13039/501100011033 and by the European Union “NextGenerationEU”/PRTR. Authors also thank Generalitat Valenciana-GVA for funding this research through the grant numbers AICO/2021/025 and CIGE/2021/094. J. Gomez-Caturla wants to thank FPU20/01732 grant funded by MCIN/AEI/10.13039/501100011033 and by ESF Investing in your future. R. Balart wants to thank “Vicerrectorado de Investigación” at Universitat Politècnica de València (UPV) for partial funding of this research through the program “Funds for First Research Projects” (PAID-06-23). Microscopy services at UPV are acknowledged for their help in using and collecting FESEM images.

Conflicts of Interest

The authors declare no conflict of interest.

Data availability statement

Data will made available on request.

References.

Almazrouei, M., Adeyemi, I., Janajreh, I., 2022. Thermogravimetric assessment of the thermal degradation during combustion of crude and pure glycerol. Biomass Conversion and Biorefinery 12, 4403-4417.

Alsadat-Seyedbokaei, F., Felix, M., Bengoechea, C., 2023. Zein as a Basis of Recyclable Injection Moulded Materials: Effect of Formulation and Processing Conditions. Polymers 15.

Alsadat-Seyedbokaei, F., Felix, M., Boengoechea, C., 2024. Effect of Recycling on Thermomechanical Properties of Zein and Soy Protein Isolate Bioplastics. Processes 12, 302.

Atta, O.M., Manan, S., Ul-Islam, M., Ahmed, A.A.Q., Ullah, M.W., Yang, G., 2022. Development and characterization of plant oil-incorporated carboxymethyl cellulose/bacterial cellulose/glycerol-based antimicrobial edible films for food packaging applications. Advanced Composites and Hybrid Materials 5, 973-990.

Bangi, U.K.H., Gafari, R.S., Pawar, R.C., Jung, H.-N.-R., Park, H.-H., 2020. Influence of Glycerol Additive on the Chemical Structure, Hydrophobicity, Morphology and Optical Properties of Sol-gel Based Zirconia Coatings. ES Materials & Manufacturing.

Barth, A., 2007. Infrared spectroscopy of proteins. Biochimica Et Biophysica Acta-Bioenergetics 1767, 1073-1101.

Biswas, A., Selling, G.W., Woods, K.K., Evans, K., 2009. Surface modification of zein films. Industrial Crops and Products 30, 168-171.

Bouman, J., Belton, P., Venema, P., van der Linden, E., de Vries, R., Qi, S., 2015. The Development of Direct Extrusion-Injection Moulded Zein Matrices as Novel Oral Controlled Drug Delivery Systems. Pharmaceutical Research 32, 2775-2786.

Bouman, J., Belton, P., Venema, P., van der Linden, E., de Vries, R., Qi, S., 2016. Controlled Release from Zein Matrices: Interplay of Drug Hydrophobicity and pH. Pharm Res 33, 673-685.

Cai, S.W., Singh, B.R., 1999. Identification of β-turn and random coil amide III infrared bands for secondary structure estimation of proteins. Biophysical Chemistry 80, 7-20.

Cai, S.W., Singh, B.R., 2004. A distinct utility of the amide III infrared band for secondary structure estimation of aqueous protein solutions using partial least squares methods. Biochemistry 43, 2541-2549.

Calvez, J., Benoit, S., Piedcoq, J., Khodorova, N., Azzout-Marniche, D., Tomé, D., Benamouzig, R., Airinei, G., Gaudichon, C., 2021. Very low ileal nitrogen and amino acid digestibility of zein compared to whey protein isolate in healthy volunteers. American Journal of Clinical Nutrition 113, 70-82.

Cao, Y., Zhu, M., Rong, M.Z., Zhang, M.Q., 2023. Injection moldable, self-healable, and recyclable rubber-bonded NdFeB magnets with the magnetic particulates content up to 90 wt%. Advanced Composites and Hybrid Materials 6.

Chen, Y., Ye, R., Li, X.M., Wang, J.Y., 2013. Preparation and characterization of extruded thermoplastic zein-poly(propylene carbonate) film. Industrial Crops and Products 49, 81-87.

Chen, Y., Ye, R., Liu, J., 2014. Effects of different concentrations of ethanol and isopropanol on physicochemical properties of zein-based films. Industrial Crops and Products 53, 140-147.

Comission Internationale de l'Eclaraige, 1977. CIE Recommendations on Uniform Color Spaces, Color-Difference Equations, and Metric Color Terms. Color Research and Application. 2, 5-6.

Corradini, E., de Medeiros, E.S., Carvalho, A.J.F., Curvelo, A.A.S., Mattoso, L.H.C., 2006. Mechanical and morphological characterization of starch/zein blends plasticized with glycerol. Journal of Applied Polymer Science 101, 4133-4139.

Cui, B., Li, J., Lai, Z.Y., Gao, F., Zeng, Z.H., Zhao, X., Liu, G.Q., Cui, H.X., 2021. Emamectin benzoate-loaded zein nanoparticles produced by antisolvent precipitation method. Polymer Testing 94.

de Almeida, C.B., Corradini, E., Forato, L.A., Fujihara, R., Lopes, J.F., 2018. Microstructure and thermal and functional properties of biodegradable films produced using zein. Polimeros-Ciencia E Tecnologia 28, 30-37.

De Marco, I., 2022. Zein Microparticles and Nanoparticles as Drug Delivery Systems. Polymers 14.

Di Maio, E., Mali, R., Iannace, S., 2010. Investigation of Thermoplasticity of Zein and Kafirin Proteins: Mixing Process and Mechanical Properties. Journal of Polymers and the Environment 18, 626-633.

Escamilla-García, M., Calderón-Domínguez, G., Chanona-Pérez, J.J., Farrera-Rebollo, R.R., Andraca-Adame, J.A., Arzate-Vázquez, I., Mendez-Mendez, J.V., Moreno-Ruiz, L.A., 2013. Physical and structural characterisation of zein and chitosan edible films using nanotechnology tools. International Journal of Biological Macromolecules 61, 196-203.

Ghalei, S., Asadi, H., Ghalei, B., 2018. Zein nanoparticle-embedded electrospun PVA nanofibers as wound dressing for topical delivery of anti-inflammatory diclofenac. Journal of Applied Polymer Science 135.

Ghanbarzadeh, B., Oromiehi, A.R., 2009. Thermal and mechanical behavior of laminated protein films. Journal of Food Engineering 90, 517-524.

Ghanbarzadeh, B., Oromiehie, A., Musavi, M., Rezayi, K., Razmi, E., Milani, J., 2006. Investigation of water vapour permeability hydrophobicity and morphology of zein films plasticized by polyols. Iranian Polymer Journal 15, 691-700.

Gianazza, E., Viglienghi, V., Righetti, P.G., Salamini, F., Soave, C., 1977. Amino-acid composition of zein molecular components. Phytochemistry 16, 315-317.

Gillgren, T., Barker, S.A., Belton, P.S., Georget, D.M.R., Stading, M., 2009. Plasticization of Zein: A Thermomechanical, FTIR, and Dielectric Study. Biomacromolecules 10, 1135-1139.

Giteru, S.G., Ali, M.A., Oey, I., 2021. Recent progress in understanding fundamental interactions and applications of zein. Food Hydrocolloids 120.

Han, T., Chen, W.X., Zhong, Q.P., Chen, W.J., Xu, Y.P., Wu, J.W., Chen, H.M., 2023. Development and Characterization of an Edible Zein/Shellac Composite Film Loaded with Curcumin. Foods 12.

Huo, W.Z., Wei, D.W., Zhu, W., Li, Z.X., Jiang, Y.B., 2018. High-elongation zein films for flexible packaging by synergistic plasticization: Preparation, structure and properties. Journal of Cereal Science 79, 354-361.

Jaski, A.C., Schmitz, F., Horta, R.P., Cadorin, L., da Silva, B.J.G., Andreaus, J., Paes, M.C.D., Riegel-Vidotti, I.C., Zimmermann, L.M., 2022. Zein - a plant-based material of growing importance: New perspectives for innovative uses. Industrial Crops and Products 186.

Jiang, L.W., Ye, R., Xie, C.C., Wang, F.H., Zhang, R., Tang, H.J., He, Z.C., Han, J.C., Liu, Y.Z., 2023a. Development of zein edible films containing different catechin/cyclodextrin metal-organic frameworks: Physicochemical characterization, antioxidant stability and release behavior. Lwt-Food Science and Technology 173.

Jiang, W., Du, Y., Huang, C., Ji, Y., Yu, D.-G., 2023b. Electrospun Zein Nanofibers: From Food to Food. ES Food & Agroforestry.

Jiao, Y., Chen, H.D., Han, H., Chang, Y., 2022. Development and Utilization of Corn Processing by-Products: A Review. Foods 11.

Kasaai, M.R., 2018. Zein and zein -based nano-materials for food and nutrition applications: A review. Trends in Food Science & Technology 79, 184-197.

Kaushik, P., Rawat, K., Aswal, V.K., Kohlbrecher, J., Bohidar, H.B., 2019. Fluorescent complex coacervates of agar and in situ formed zein nanoparticles: Role of electrostatic forces. Carbohydrate Polymers 224.

Kuang, T., Ju, J., Liu, T., Hejna, A., Saeb, M.R., Zhang, S., Peng, X., 2022. A facile structural manipulation strategy to prepare ultra-strong, super-tough, and thermally stable polylactide/nucleating agent composites. Advanced Composites and Hybrid Materials 5, 948-959.

Lawton, J.W., 2004. Plasticizers for zein: Their effect on tensile properties and water absorption of zein films. Cereal Chemistry 81, 1-5.

Lenzuni, M., Fiorentini, F., Summa, M., Bertorelli, R., Suarato, G., Perotto, G., Athanassiou, A., 2024. Electrosprayed zein nanoparticles as antibacterial and anti-thrombotic coatings for ureteral stents. International Journal of Biological Macromolecules 257.

Li, Z., Li, Y., Lei, H., Feng, Y., Wang, W., Li, J., Ding, T., Yuan, B., 2022. The effect of synergistic/inhibitory mechanism of terephthalic acid and glycerol on the puncture, tearing, and degradation properties of PBSeT copolyesters. Advanced Composites and Hybrid Materials 5, 1335-1349.

Liang, J., Xia, Q.Y., Wang, S.M., Li, J., Huang, Q.R., Ludescher, R.D., 2015. Influence of glycerol on the molecular mobility, oxygen permeability and microstructure of amorphous zein films. Food Hydrocolloids 44, 94-100.

Lim, S., Jane, J., 1994. Storage stability of injection-molded starch-zein plastics under dry and humid conditions. Journal of Environmental Polymer Degradation 2, 111-120.

Liu, Q., Chen, Z., El-Bahy, Z.M., Wang, P., Abdou, S.N., Ibrahim, M.M., Wan, Y., Wang, J., Li, H., Li, L., Wang, H., 2023. Alkali-hydrothermal activation of tailings with red mud as a supplementary alkali source to synthesize one-part geopolymer. Advanced Composites and Hybrid Materials 6.

Liu, W., Qiu, J., Fei, M., Qiu, R., Sakai, E., Zhang, M., 2019. Balancing performance of epoxidized soybean oil (ESO)/poly(lactic acid) composites: Synergistic effects of carbon nanotubes and tannic acid-induced crosslinking of ESO. Express Polymer Letters 13, 109-122.

Liu, X., Wu, Z., Jiang, D., Guo, N., Wang, Y., Ding, T., Weng, L., 2022. A highly stretchable, sensing durability, transparent, and environmentally stable ion conducting hydrogel strain sensor built by interpenetrating Ca2+-SA and glycerol-PVA double physically cross-linked networks. Advanced Composites and Hybrid Materials 5, 1712-1729.

Luo, Y.C., Wang, Q., 2014. Zein-Based Micro- and Nano-Particles for Drug and Nutrient Delivery: A Review. Journal of Applied Polymer Science 131.

Martin, A., Cai, J., Schaedel, A.L., van der Plas, M., Malmsten, M., Rades, T., Heinz, A., 2022. Zein-polycaprolactone core-shell nanofibers for wound healing. International Journal of Pharmaceutics 621.

Masanabo, M.A., Ray, S.S., Emmambux, M.N., 2022. Properties of thermoplastic maize starch-zein composite films prepared by extrusion process under alkaline conditions. International Journal of Biological Macromolecules 208, 443-452.

Mattice, K.D., Marangoni, A.G., 2020. Evaluating the use of zein in structuring plant-based products. Current Research in Food Science 3, 59-66.

Mojica-Munoz, D.M., Macias-Sanchez, K.L., Juarez-Hernandez, E.O., Rodriguez-Alvarez, A., Grevy, J.M., Diaz-Valle, A., Carrillo-Tripp, M., Falcon-Gonzalez, J.M., 2024. Optimizing biodegradable plastics: Molecular dynamics insights into starch plasticization with glycerol and oleic acid. J Mol Graph Model 126, 108674.

Nunes, R., Baiao, A., Monteiro, D., das Neves, J., Sarmento, B., 2020. Zein nanoparticles as low-cost, safe, and effective carriers to improve the oral bioavailability of resveratrol. Drug Delivery and Translational Research 10, 826-837.

Oliviero, M., Di Maio, E., Iannace, S., 2010. Effect of Molecular Structure on Film Blowing Ability of Thermoplastic Zein. Journal of Applied Polymer Science 115, 277-287.

Özeren, H.D., Olsson, R.T., Nilsson, F., Hedenqvist, M.S., 2020. Prediction of plasticization in a real biopolymer system (starch) using molecular dynamics simulations. Materials & Design 187.

Özeren, H.D., Wei, X.-F., Nilsson, F., Olsson, R.T., Hedenqvist, M.S., 2021. Role of hydrogen bonding in wheat gluten protein systems plasticized with glycerol and water. Polymer 232.

Pascoli, M., de Lima, R., Fraceto, L.F., 2018. Zein Nanoparticles and Strategies to Improve Colloidal Stability: A Mini-Review. Frontiers in Chemistry 6.

Peña-Bahamonde, J., Herrera, G., Lupini, S., Arabaghian, H., Rodrigues, D.F., 2023. Zein Nanoparticles for Controlled Intestinal Drug Release for the Treatment of Gastrointestinal Infections. Acs Applied Nano Materials 6, 21707-21720.

Pérez-Guzmán, C.J., Castro-Muñoz, R., 2020. A Review of Zein as a Potential Biopolymer for Tissue Engineering and Nanotechnological Applications. Processes 8.

Qin, M., Mou, X.J., Dong, W.H., Liu, J.X., Liu, H., Dai, Z., Huang, X.W., Wang, N., Yan, X., 2020. In Situ Electrospinning Wound Healing Films Composed of Zein and Clove Essential Oil. Macromolecular Materials and Engineering 305.

Raza, A., Hayat, U., Bilal, M., Iqbal, H.M.N., Wang, J.Y., 2020. Zein-based micro-and nano-constructs and biologically therapeutic cues with multi-functionalities for oral drug delivery systems. Journal of Drug Delivery Science and Technology 58.

Sánchez, A.C., Popineau, Y., Mangavel, C., Larré, C., Guéguen, J., 1998. Effect of Different Plasticizers on the Mechanical and Surface Properties of Wheat Gliadin Films. Journal of Agricultural and Food Chemistry 46, 4539-4544.

Selling, G.W., 2010. The effect of extrusion processing on Zein. Polymer Degradation and Stability 95, 2241-2249.

Selling, G.W., Woods, K.K., Biswas, A., Willett, J.L., 2009. Reactive Extrusion of Zein with Glyoxal. Journal of Applied Polymer Science 113, 1828-1835.

Sessa, D.J., Woods, K.K., Mohamed, A.A., Palmquist, D.E., 2011. Melt-processed blends of zein with polyvinylpyrrolidone. Industrial Crops and Products 33, 57-62.

Shi, K., Kokini, J.L., Huang, Q.R., 2009. Engineering Zein Films with Controlled Surface Morphology and Hydrophilicity. Journal of Agricultural and Food Chemistry 57, 2186-2192.

Spasojevic, L., Katona, J., Bucko, S., Savic, S.M., Petrovic, L., Budinicic, J.M., Tasic, N., Aidarova, S., Sharipova, A., 2019. Edible water barrier films prepared from aqueous dispersions of zein nanoparticles. Lwt-Food Science and Technology 109, 350-358.

Sun, Y., Liu, Z.L., Zhang, L.M., Wang, X.M., Li, L., 2020. Effects of plasticizer type and concentration on rheological, physico-mechanical and structural properties of chitosan/zein film. International Journal of Biological Macromolecules 143, 334-340.

Tadele, D.T., Shorey, R., Mekonnen, T.H., 2023. Fatty acid modified zein films: Effect of fatty acid chain length on the processability and thermomechanical properties of modified zein films. Industrial Crops and Products 192, 12.

Tavares-Negrete, J.A., Aceves-Colin, A.E., Rivera-Flores, D.C., Díaz-Armas, G.G., Mertgen, A.S., Trinidad-Calderon, P.A., Olmos-Cordero, J.M., Gómez-López, E.G., Pérez-Carrillo, E., Escobedo-Avellaneda, Z.J., Tamayol, A., Alvarez, M.M., Trujillo-de Santiago, G., 2021. Three-Dimensional Printing Using a Maize Protein: Zein-Based Inks in Biomedical Applications. Acs Biomaterials Science & Engineering 7, 3964-3979.

Trujillo-de Santiago, G., Rojas-de Gante, C., García-Lara, S., Verdolotti, L., Di Maio, E., Iannace, S., 2014. Strategies to Produce Thermoplastic Starch–Zein Blends: Effect on Compatibilization. Journal of Polymers and the Environment 22, 508-524.

Wang, L., Zhang, Y., 2019. Heat-induced self-assembly of zein nanoparticles: Fabrication, stabilization and potential application as oral drug delivery. Food Hydrocolloids 90, 403-412.

Wang, Y., Padua, G.W., 2003. Tensile properties of extruded Zein sheets and extrusion blown films. Macromolecular Materials and Engineering 288, 886-893.

Wang, Y., Rakotonirainy, A.M., Padua, G.W., 2003. Thermal behavior of zein-based biodegradable films. Starch-Starke 55, 25-29.

Wang, Y.H., Wang, J.M., Yang, X.Q., Guo, J., Lin, Y., 2015. Amphiphilic zein hydrolysate as a novel nano-delivery vehicle for curcumin. Food & Function 6, 2636-2645.

Wang, Z., Li, R., Zhang, J., 2022. On-demand drug delivery of triptolide and celastrol by poly(lactic-co-glycolic acid) nanoparticle/triglycerol monostearate-18 hydrogel composite for rheumatoid arthritis treatment. Advanced Composites and Hybrid Materials 5, 2921-2935.

Wongsasulak, S., Tongsin, P., Intasanta, N., Yoovidhya, T., 2010. Effect of glycerol on solution properties governing morphology, glass transition temperature, and tensile properties of electrospun zein film. Journal of Applied Polymer Science 118, 910-919.

Wu, F., Wei, J., Liu, C.S., O'Neill, B., Ngothai, Y., 2012. Fabrication and properties of porous scaffold of zein/PCL biocomposite for bone tissue engineering. Composites Part B-Engineering 43, 2192-2197.

Xu, H., Chai, Y.W., Zhang, G.Y., 2012. Synergistic Effect of Oleic Acid and Glycerol on Zein Film Plasticization. Journal of Agricultural and Food Chemistry 60, 10075-10081.

Xu, J., Liu, R., Wang, L., Pranovich, A., Hemming, J., Dai, L., Xu, C., Si, C., 2023. Towards a deep understanding of the biomass fractionation in respect of lignin nanoparticle formation. Advanced Composites and Hybrid Materials 6.

Yilmaz, M.T., Kul, E., Saricaoglu, F.T., Odabas, H.I., Taylan, O., Dertli, E., 2024. Deep eutectic solvent as plasticizing agent for the zein based films. Food Packaging and Shelf Life 42, 101252.

Zhang, D.C., Jiang, F.Y., Ling, J.H., Ouyang, X.K., Wang, Y.G., 2021a. Delivery of curcumin using a zein-xanthan gum nanocomplex: Fabrication, characterization, and in vitro release properties. Colloids and Surfaces B-Biointerfaces 204.

Zhang, L.M., Liu, Z.L., Sun, Y., Wang, X.M., Li, L., 2020. Effect of α-tocopherol antioxidant on rheological and physicochemical properties of chitosan/zein edible films. Lwt-Food Science and Technology 118.

Zhang, X.R., Dong, C.X., Hu, Y.Y., Gao, M.N., Luan, G.Z., 2021b. Zein as a structural protein in gluten-free systems: an overview. Food Science and Human Wellness 10, 270-277.

Zhou, L.P., Wang, Y., 2021. Physical and antimicrobial properties of zein and methyl cellulose composite films with plasticizers of oleic acid and polyethylene glycol. Lwt-Food Science and Technology 140.